Electronic Supplementary Information to:

π-Stacked Poly(vinyl ketone)s with Accumulated Push-pull Triphenylamine Moieties in the Side Chain

Heng Wang,[†, ‡] Yue Wang,[†] Xichong Ye,[†, §] Haruka Hayama,[†, ∥] Hiroyoshi Sugino,[†] Hideyuki Nakano,[⊥] and Tamaki Nakano[†,#,*]

[†]Macromolecular Science Research Division, Institute for Catalysis (ICAT), Hokkaido University, N21, W10, Kita-ku, Sapporo 001-0021, Japan,

[∥]Graduate School of Chemical Sciences and Engineering, Hokkaido University, N21, W10, Kita-ku, Sapporo 001-0021, Japan.

[⊥]Department of Applied Chemistry, Muroran Institute of Technology, Mizumoto-cho, Muroran, Hokkaido 050-8585, Japan

[#]Integrated Research Consortium on Chemical Sciences (IRCCS), Institute for Catalysis, Hokkaido University, N21 W10, Kita-ku, Sapporo 001-0021, Japan

[§]Visiting scientist at Hokkaido University on leave from College of Chemistry & Molecular Engineering, Peking University.

*Correspondence to Tamaki Nakano (tamaki.nakano@cat.hokudai.ac.jp)

Table of contents

Experimental

Materials. 4,4'-Dimethyltriphenylamine (Kanto Chemical), methacryloyl chloride (TCI), pivaloyl chloride (TCI), aluminum(Ⅲ) chloride (Kanto Chemical), tri-*n*-butylborane in a THF solution (1.0 M) (Aldrich) and 2,6-di-*t*-butyl-*p*-cresol (BHT) (Wako) were used as purchased. Dichloromethane (Kanto Chemical) and tetrahydrofuran (THF) (Kanto Chemical) were dried over CaH_2 and sodium metal, respectively, distilled, and stored under N_2 atmosphere. Styrene (St) (99%, stabilized with 30 ppm *p-t*-butyl catechol, Wako) was washed three times with 5% aq. KOH, three times with distilled water, and once with brine in this order, dried with anhydrous $CaCl_2$ and distilled over CaH_2 under a reduced pressure immediately before use. α,α'-Azobisisobutyronitrile (AIBN) (TCI) was recrystallized from an ethanol solution twice and dried under vacuum before use.

Measurements. NMR spectra were recorded on JEOL JMN-ECX400 (400 MHz for ^{1}H, 100 MHz for ^{13}C) and JEOL JMN-ECX600 (600 MHz for ^{1}H, 125 MHz for ^{13}C) spectrometers. Size-exclusion chromatography (SEC) measurements were carried out using a chromatographic system consisting of a JASCO DG-980-50 degasser, a HITACHI L-7100 pump, a HITACHI L-7420 UV-Vis detector and a HITACHI L-7490 RI detector, equipped with TOSOH TSKgel G3000H HR and G6000H HR columns (30 × 0.72 (i.d.) cm) connected in series (eluent: THF, flow rate: 1.0 mL/min). Preparative recycling SEC was performed with a JAI LC-9201 chromatograph consisting of a JAI PI-50 pump and a Soma S-3740 UV/Vis detector equipped with JAIGEL 1H and 2H columns (60 × 2 (i.d.) cm) connected in series (eluent: $CHCl_3$, rate: 3.5 mL/min). UV-Vis spectra were taken using quartz cells on JASCO V-550 and V-570 spectrophotometers, and fluorescence spectra were measured using quartz cells on a JASCO PF-8500 fluorescence spectrophotometer. Cyclic voltammetry was performed with an ALS/CH Instruments 630C electrochemical analyzer using Pt electrodes. Dynamic light scattering (DLS) measurements were conducted using a Nicomp 380 ZLS particle sizing system equipped with a 532-nm diode laser. Samples were introduced in a 1-cm square quartz cell, and scattering at an angle of 90º with respect to the incident light beam was detected.

Synthesis of isopropenyl 4-[bis(4-methylphenyl)amino]phenyl ketone (IMAPK) (1-[bis(4-methylphenyl)amino]phenyl-2-methylprop-2-en-1-one) (method 1). CH_2Cl_2 (8 mL) and methacryloyl chloride (0.32 mL, 3.0 mmol) were introduced to a flask containing 4,4'-dimethyltriphenylamine (520 mg, 1.9 mmol), 2,6-di-*t*-butyl-4-methylphenol (42 mg, 0.19 mmol), and aluminum(Ⅲ) chloride (405 mg, 3.0 mmol). The reaction mixture was refluxed for 21 hours under N_2 atmosphere in the dark. The mixture was poured into ice-water under vigorous stirring, and the organic layer was separated. The aqueous layer was extracted with CH_2Cl_2 (3 × 10 mL). The combined organic layer was washed twice with brine, dried over anhydrous $MgSO_4$ and filtered. The crude product obtained by concentrating the filtrate was subjected to column chromatography first using alkaline Al_2O_3 with a CH_2Cl_2-hexane (1/3, v/v) mixture as eluent and then further with silica gel using a CH_2Cl_2-hexane (1/6, v/v) mixture to afford IMAPK as a yellow amorphous (337 mg, 52%).

^{1}H NMR (400 MHz, $CDCl_3$, δ/ppm): 7.65 (d, *J* = 8.9 Hz, 2H), 7.12 (d, *J* = 8.4 Hz, 4H), 7.05 (d, *J* = 8.4 Hz, 4H), 6.91 (d, *J* = 8.9 Hz, 2H), 5.73 (m, 1H), 5.52 (m, 1H), 2.34 (s, 6H), 2.05 (m, 3H); ^{13}C NMR (150 MHz, $CDCl_3$, δ/ppm): 196.8, 152.0, 143.9, 134.3, 131.3, 130.2, 128.5, 126.0, 123.6, 118.4, 20.9, 19.3; IR (neat) v/cm[-1]: 3027, 2921, 1647, 1591, 1507, 1450, 1427, 1322, 1296, 1211,

1166, 1109, 1021, 981, 932, 904, 846, 816, 764, 721, 707; LR-MS (ESI) *m/z* (%): 364 (100, [M+Na]$^+$), 342 (50, [M+H]$^+$), 196 (48, [M−(C$_4$H$_6$-COC(CH$_2$)CH$_3$)]$^+$); HR-MS (ESI) calcd. For C$_{24}$H$_{23}$ONNa: 364.16719; found: 364.16725.

Synthesis of isopropenyl 4-[bis(4-methylphenyl)amino]phenyl ketone (IMAPK) (1-[bis(4-methylphenyl)amino]phenyl-2-methylprop-2-en-1-one) (method 2). Aluminum(III) chloride (405 mg, 3.0 mmol) was added to a solution of 4,4'-dimethyltriphenylamine (520 mg, 1.9 mmol) and methacryloyl chloride (318 μL, 3.0 mmol) in CH$_2$Cl$_2$ (10 mL). The mixture was refluxed for 21 h under N$_2$ atmosphere in the dark. The reaction mixture was poured into ice-water, and the organic layer was separated from the aqueous layer. The aqueous layer was extracted with CH$_2$Cl$_2$. The combined organic layer was dried over MgSO$_4$ and then filtered. The crude product obtained by concentrating the filtrate was subjected to column chromatography (SiO$_2$, CH$_2$Cl$_2$) to give **IMAPK** as an orange amorphous (428 mg, 66%).

^{1}H NMR (400 MHz, CDCl$_3$) δ/ppm: 7.65 (d, *J* = 8.9 Hz, 2H), 7.12 (d, *J* = 8.4 Hz, 4H), 7.05 (d, *J* = 8.4 Hz, 4H), 6.91 (d, *J* = 8.9 Hz, 2H), 5.73 (t, *J* = 1.4 Hz, 1H), 5.52 (t, *J* = 1.0 Hz, 1H), 2.34 (s, 6H), 2.05 (dd, *J* = 1.0, 1.4 Hz, 3H); IR (KBr) υ/cm^{-1}: 3027, 2921, 1647, 1591, 1507, 1450, 1427, 1322, 1296, 1211, 1166, 1109, 1021, 981, 932, 904, 846, 816, 764, 721, 707.

Synthesis of *t*-butyl 4-[bis(4-methylphenyl)amino]phenyl ketone (BMAPK) (1-[bis(4-methylphenyl)amino]phenyl-2,2-dimethylpropan-1-one). CH$_2$Cl$_2$ (8 mL) and pivaloyl chloride (0.37 mL, 3.0 mmol) were introduced to a flask containing 4,4'-dimethyltriphenylamine (520 mg, 1.9 mmol), and aluminum (III) chloride (405 mg, 3.0 mmol). The reaction mixture was refluxed for 24 hours under N$_2$ atmosphere in the dark. The mixture was poured into ice-water under vigorous stirring, and the organic layer was separated. The aqueous layer was extracted with CH$_2$Cl$_2$ (3 × 10 mL). The combined organic layer was washed twice with brine, dried over anhydrous MgSO$_4$ and filtered. The crude product obtained by concentrating the filtrate was subjected to silica gel chromatography with two eluent systems: a CH$_2$Cl$_2$-hexane mixture (1/5, v/v) as the first eluent washed out the unreacted reagents, and pure CH$_2$Cl$_2$ as the second eluent led to elution of BMAPK. BMAKP was obtained as light yellow amorphous (240 mg, 46%).

^{1}H NMR (400 MHz, CDCl$_3$, δ/ppm): 7.73 (d, *J* = 8.9 Hz, 2H), 7.11 (d, *J* = 8.4 Hz, 4H), 7.05 (d, *J* = 8.4 Hz, 4H), 6.89 (d, *J* = 8.9 Hz, 2H), 2.33 (s, 6H), 1.36 (s, 9H); ^{13}C NMR (150 MHz, CDCl$_3$, δ/ppm): 205.5, 151.0, 144.0, 134.1, 130.5, 130.1, 128.6, 125.9, 118.4, 43.7, 28.5, 20.9; HR-MS (EI) calcd. For [C$_{25}$H$_{27}$ON]$^{+•}$: 357.20926; found:357.20934.

Radical copolymerization of IMAPK (M$_1$) with St (M$_2$). The copolymerization of IMAPK with St at M$_1$/M$_2$ = 1/1 (run 4 in Table 1) is described as an example. IMAPK (50 mg, 0.15 mmol), St (15 mg, 0.15 mmol), and AIBN (5 mg, 0.03 mmol) were dissolved in THF (0.15 mL) in a reaction tube. After three freeze-pump-thaw cycles, the tube was filled with N$_2$ and the reaction mixture was heated at 60 °C for 24 hours. After the reaction was quenched by cooling in liquid N$_2$, the mixture was dissolved in 5 mL of THF and reprecipitated into methanol (100 mL). The precipitate was collected with a centrifuge and washed three times with methanol. On drying under vacuum at r.t. for 24 hours, poly(IMAPK-co-St) was obtained as light yellow powder (25 mg, 38%).

^{1}H NMR (400 MHz, CDCl$_3$, δ ppm): 6.10-7.70 (br, protons on the phenyl groups), 2.20-2.75 (br, -N-PhC*H*$_3$), 0.22-2.20 (br, -C*H*PhC*H*$_2$-, -C(C*H*$_3$)(CO-)-C*H*$_2$-). *M*$_n$ = 1.7 ×10^3 Da, *PDI* = 1.39. The

M_1/M_2 ratio in polymer was estimated to be 1/2 from ^{1}H NMR spectra where the signals of methyl groups due to the side chain group were considered to represent the relative amount of the IMAPK units.

Radical homopolymerization of IMAPK using tri-*n*-butylborane. A solution of IMAPK (50 mg, 0.15 mmol) in THF (50 μL) was prepared in a reaction tube under N_2 atmosphere through three freeze-pump-thaw cycles. After the addition of *n*-Bu$_3$B (15 μL, 0.015 mmol) in a THF solution (1 mol/L) to the reaction system with a syringe, the mixture was cooled at −78 °C. Air (0.2 mL, containing ca. 1.5 μmol oxygen) was slowly bubbled into the mixture to initiate the polymerization, and the reaction system was warmed to room temperature after 48 hours of polymerization. The mixture was dissolved in 5 mL of THF and reprecipitated in MeOH (25 mL). The precipitate was collected with a centrifuge and washed three times with fresh methanol. On vacuum drying, poly(IMAPK) was obtained as yellow powder was obtained (3 mg, 6%).

^{1}H NMR (400 MHz, CDCl$_3$, δ ppm): 6.55-7.16 (br, 12H, protons on the phenyl groups), 2.09-2.40 (br, 6H, -N-PhC*H*$_3$), 1.11-1.36 (br, 3H, -C(C*H*$_3$)(COPh)-CH$_2$-), 0.78-0.93 (br, 2H, -C(CH$_3$)(COPh)-C*H*$_2$-). $M_n = 6.2 \times 10^2$ Da, $PDI = 1.05$.

Theoretical Calculations. Molecular geometries of all the compounds were fully optimized by Kohn-Sham DFT based on the Becke's three-parameter hybrid functional (B3LYP) with the 6-311G(d, p) basis set using the Gaussian 09 program package. Each optimization was verified by frequency analysis. The ground-state conformation was optimized, and the corresponding molecular orbital (MO) energy levels were calculated by the DFT method. The excited-state conformation and MO energy levels were calculated by the TD-DFT method.

Table S1. Radical copolymerization of IMAPK (M_1) with St (M_2) using AIBN as initiator at 60 ºC[a]

Run	M_1	M_2	$[M_1]/[M_2]$ in feed	Conv. of M_1[c]	Conv. of M_2[c]	MeOH-insoluble Polymer			
						Yield[d]	M_n[e]	M_w/M_n[e]	M_1/M_2[f]
1[b]	IMAPK	St	1/4	23%	23%	21%	5300	2.36	1/4
2	IMAPK	St	1/4	71%	85%	71%	3000	1.62	1/5
3	IMAPK	St	1/1	58%	86%	38%	1700	1.39	1/2
4	IMAPK	St	4/1	36%	82%	10%	1300	1.18	2/1
5	IMAPK	–	–	< 2%	–	0%	–	–	–
6[b]	–	St	–	–	66%	52%	8000	1.64	–
7	–	St	–	–	86%	69%	2900	1.44	–

[a]Polymerization conditions: $[M_1 + M_2] = 2$ mol/L; initiator, $[M_1 + M_2]/[AIBN] = 10/1$; temperature, 60 °C; time, 24h; in dark. [b]$[M_1 + M_2]/[AIBN] = 100/1$. [c]Determined by ^{1}H NMR analysis of crude product. [d]Precipitated in methanol and collected with a centrifuge. [e]Determined by SEC on the basis of polystyrene standards (eluent: THF). [f]Determined by ^{1}H NMR analysis of purified product with methyl protons on tolyl groups of IMAPK as standard (δ: 2.0~2.5 ppm).

Table S2. Electrochemical and spectrophotometric characteristics of IMAPK, BMAPK and the polymers.

Samples	$E_{1/2}^{1}$[a] (V)	$E_{1/2}^{2}$[a] (V)	E_{ox}^{onset}[b] (V)	E_g[c]	E_{HOMO} (eV)[d]	E_{LUMO} (eV)[e]	i_{ox1}/i_{ox2}[f]
IMAPK	–	1.04	0.86	2.94	−5.26	−2.23	–
BMAPK	–	1.04	0.96	3.09	−5.36	-2.27	–
Poly(IMAPK)	0.92	1.10	0.82	2.89	−5.22	−2.33	1.40
Poly(IMAPK-co-St) ([IMAPK]/[St] = 1/5)	0.86	1.01	0.79	3.07	−5.19	−2.12	0.32
Poly(IMAPK-co-St) ([IMAPK]/[St] = 1/2)	0.88	1.03	0.79	3.04	−5.19	−2.15	0.46
Poly(IMAPK-co-St) ([IMAPK]/[St] = 2/1)	0.88	1.03	0.80	3.00	−5.20	−2.20	0.53

[a]Half-wave potentials of the two redox signals determined in CH_2Cl_2 containing tetra-n-butylammonium hexafluorophosphate (TBAH) (0.1 M) with Ag/AgCl/KCl (saturated) as reference electrode where substrate concentration was ca. 1 mM and scan rate (υ) was 100 mV/S. [b]Estimated from the intersection of the two tangents drawn at the rising oxidation current and the background current in CV. [c]Determined on the basis of the absorption edge wavelength (λ_{onset}) in UV-Vis spectra: $E_g = 1240/\lambda_{onset}$. [d]$E_{HOMO} = -e(E_{ox}^{onset} - E_{1/2(ferrocene)} + 4.8)$ where $E_{1/2(ferrocene)} = 0.50$ V. [e]$E_{LUMO} = E_{HOMO} + E_g$. [f]The peak current ratio of the two oxidation signals.

Table S3. Absorbance and emission spectral characteristics of IMAPK, BMAPK and the polymers

Samples	Solvent	Absorbance[a]			Emission[b]		
		λ_1 (nm)	λ_2 (nm)	$\varepsilon(\lambda_1)/\varepsilon(\lambda_2)$	λ_{em} (nm)	$\lambda_{em}-\lambda_2$[c] (nm)	Φ[d]
IMAPK	Cyclohexane	294	359	1.26	424	65	0.01
	THF	292	361	1.25	492	131	0.27
	CHCl$_3$	294	371	1.45	535	164	0.06
	CH$_3$CN	290	358	1.42	557	199	0.01
BMAPK	Cyclohexane	296	347	1.58	408	61	0.03
	THF	294	348	1.46	469	121	0.58
	CHCl$_3$	297	354	1.65	505	151	0.46
	CH$_3$CN	293	343	1.56	527	184	0.13
Poly(IMAPK)	THF	302	355	0.29	474	119	0.21
	CHCl$_3$	305	363	0.29	511	148	0.12
Poly(IMAPK-co-St) ([IMAPK]/[St] = 1/5)	Cyclohexane	301	352	0.96	436	84	0.15
	THF	298	351	0.90	463	112	0.55
	CHCl$_3$	301	358	1.03	478	120	0.67
	CH$_3$CN [d]	297	348	0.83	510	162	0.27
Poly(IMAPK-co-St) ([IMAPK]/[St] = 1/2)	Cyclohexane	302	351	0.84	439	88	0.18
	THF	299	350	0.87	467	117	0.54
	CHCl$_3$	302	357	0.96	479	122	0.52
Poly(IMAPK-co-St) ([IMAPK]/[St] = 2/1)	THF	299	350	0.74	472	122	0.45
	CHCl$_3$	301	360	0.82	484	124	0.36

[a]Cell path length, 10 mm; concentration, 10^{-5} mol/L order. [b]Cell path length, 10 mm; concentration, $10^{-6} \sim 10^{-7}$ mol/L order; absorbance at 360 nm, less than 0.02 a.u. [c]Stokes shift $= \lambda_{em} - \lambda_2$. [d]Relative quantum yield is calculated from the equation:

$$\frac{\Phi_{Sample}}{\Phi_{Standard}} = \left(\frac{A_{Standard}}{A_{Sample}}\right) \times \left(\frac{F_{Sample}}{F_{Standard}}\right) \times \left(\frac{n_{Sample}^2}{n_{Standard}^2}\right) \times \left(\frac{D_{Sample}}{D_{Standard}}\right)$$

where Φ, A, F, n, and D refer to quantum yield, absorbance as 360 nm, integrated area of emission spectrum, average refractive index value of solvent, and dilution ratio, respectively, and the subscripts, "sample" and "standard", mean the sample in question and the standard sample. The standard sample in this work is 9,9-diphenylanthracene in cyclohexane ($\Phi = 0.90$).[1]

Fig. S1. ^{1}H NMR spectrum of IMAPK. [400 MHz, CDCl$_3$, TMS, room temp.]

Fig. S2. ^{13}C NMR spectrum of IMAPK. [100 MHz, CDCl$_3$, room temp.]
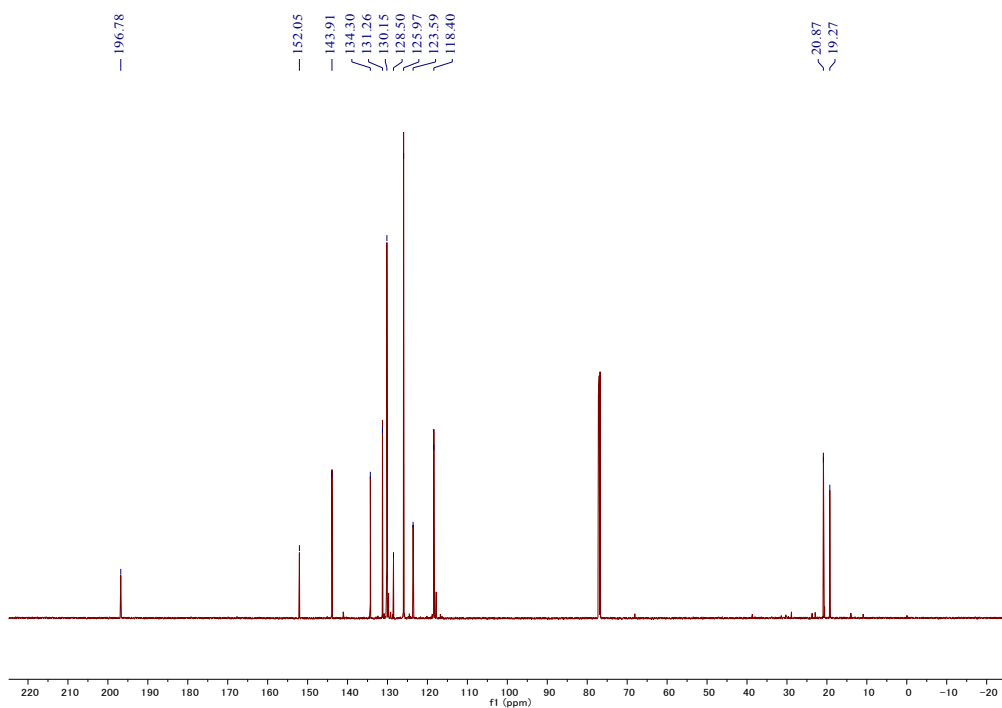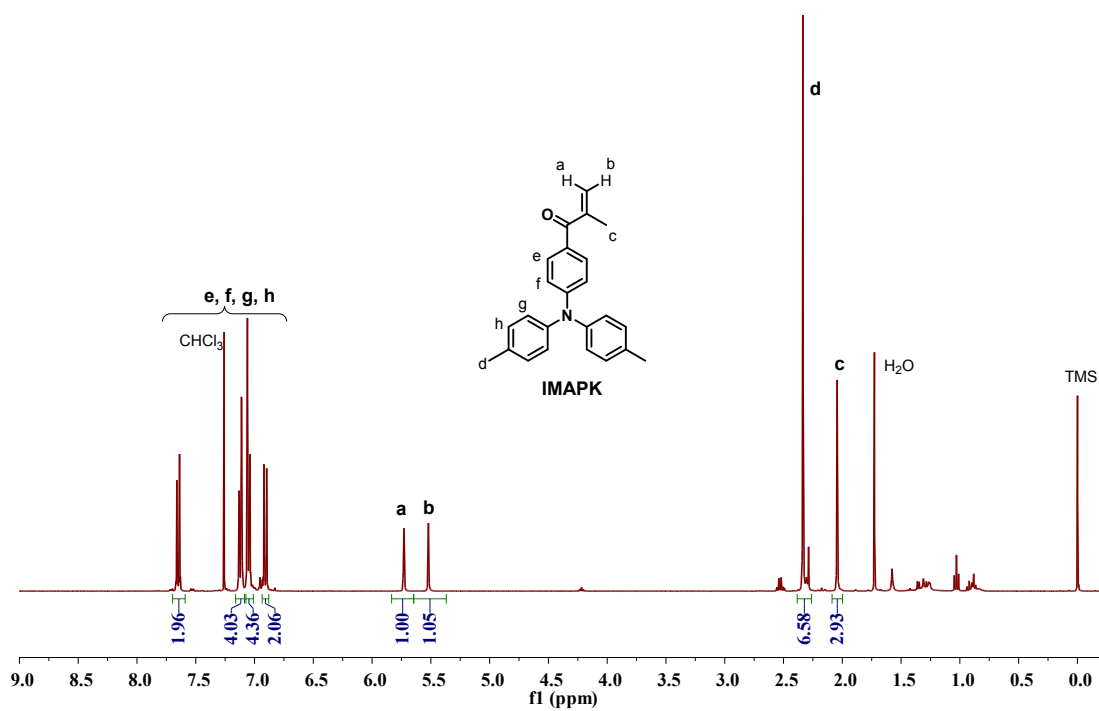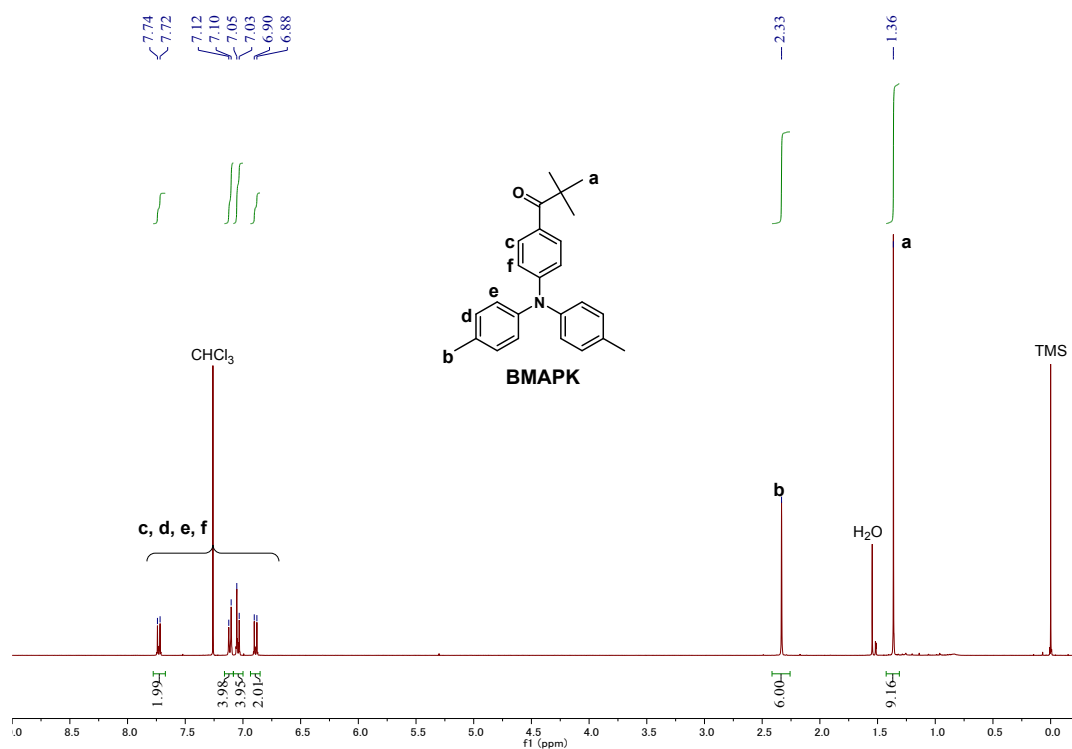
Fig. S3. ^{1}H NMR spectrum of BMPAK. [400 MHz, CDCl$_3$, TMS, room temp.]
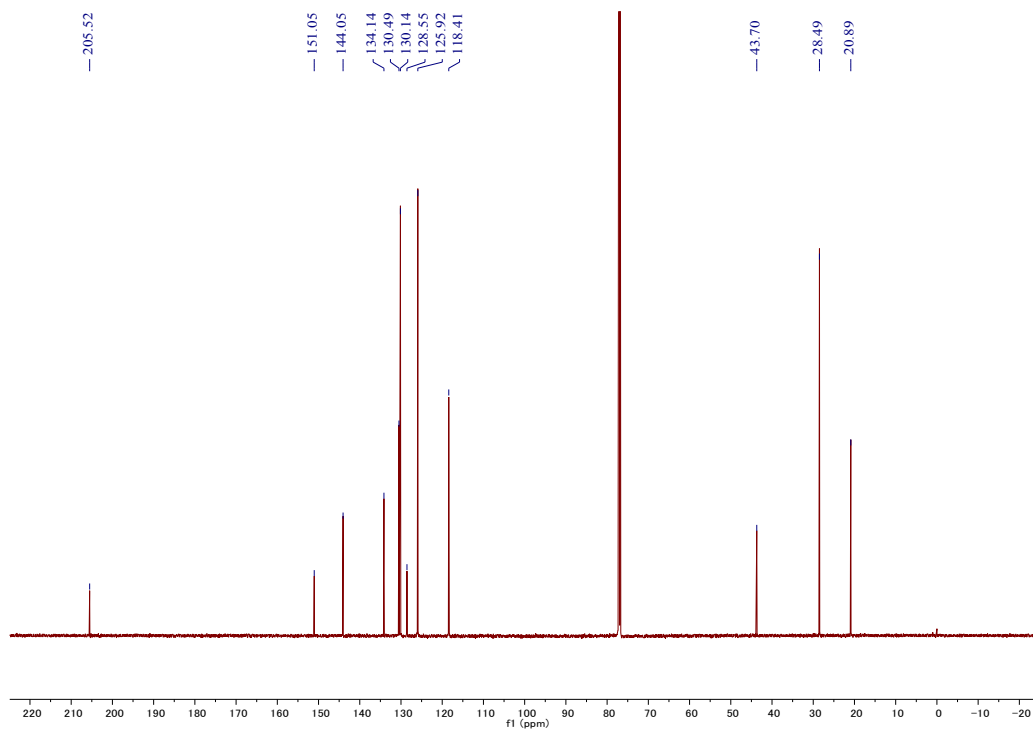
Fig. S4. ^{13}C NMR spectrum of BMPAK. [100 MHz, CDCl$_3$, room temp.]
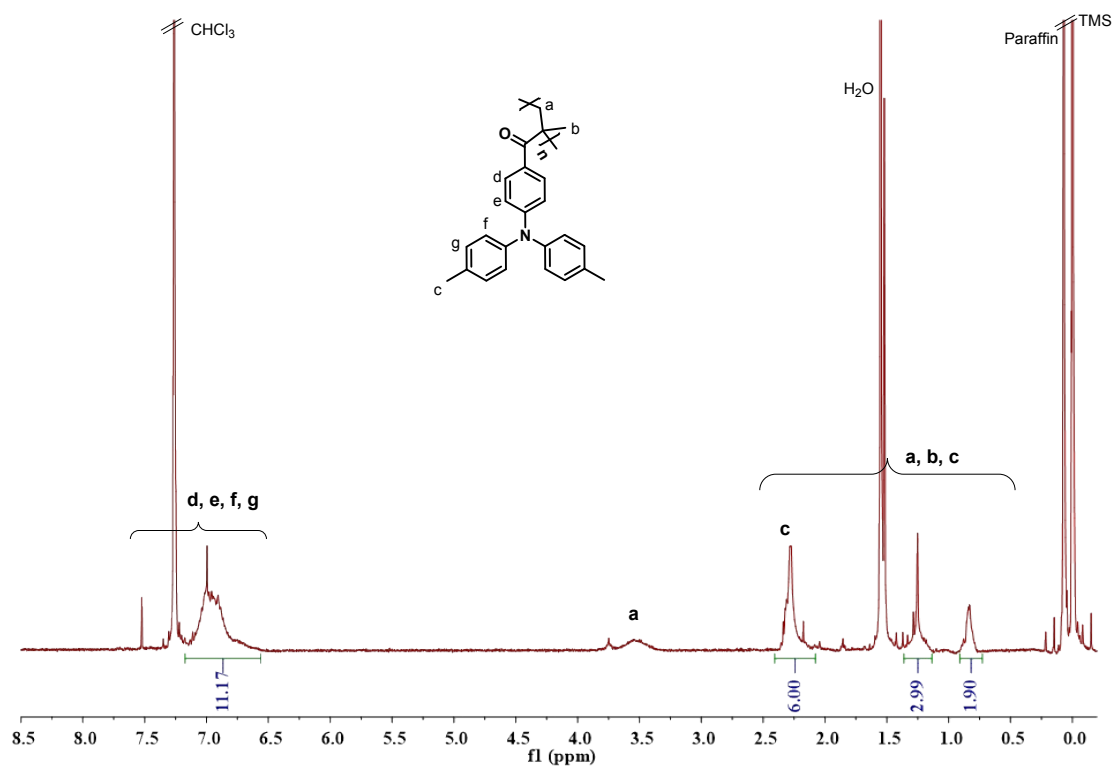
Fig. S5. ^{1}H NMR of poly(IMAPK) obtained by homopolymerization in THF at −78 °C initiated by tri(*n*-butyl)borane. [400 MHz, CDCl$_3$, TMS, room temp.]

A
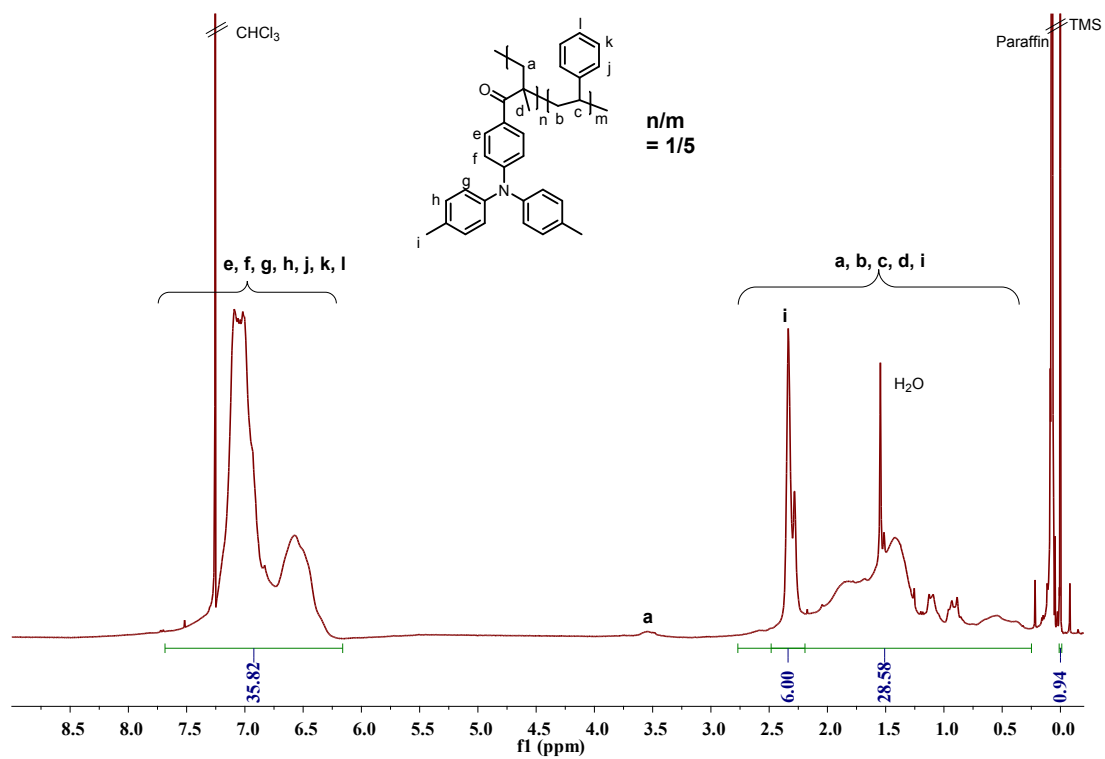
B
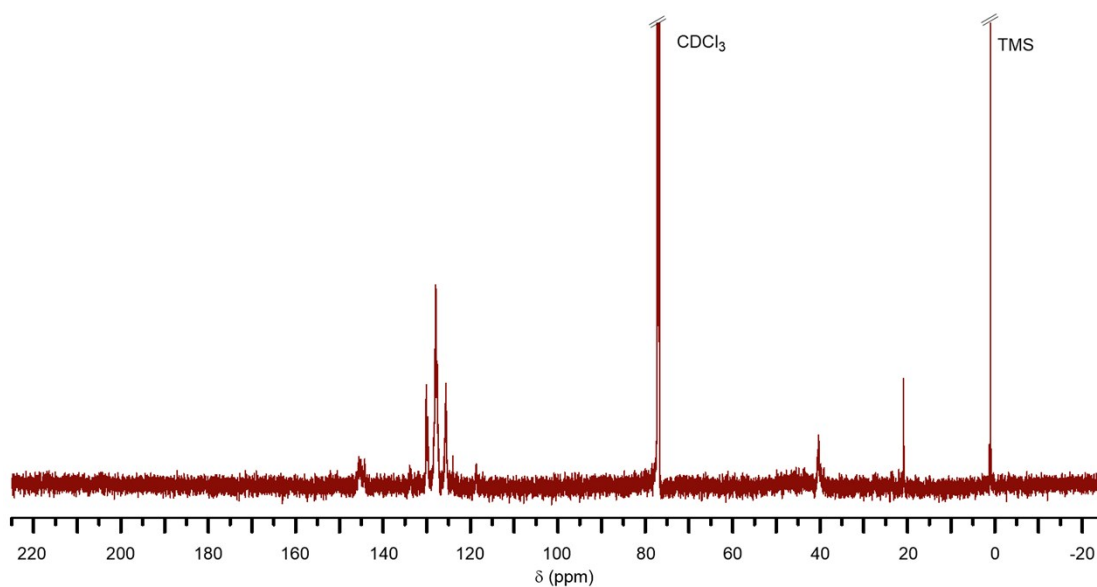
Fig. S6. ¹H NMR (A) and ¹³C NMR (B) spectra of poly(IMAPK-co-St) ([IMAPK]/[St] =1/5 in polymer). [400 MHz (¹H), 125 MHz (¹³C), CDCl₃, TMS, room temp.]
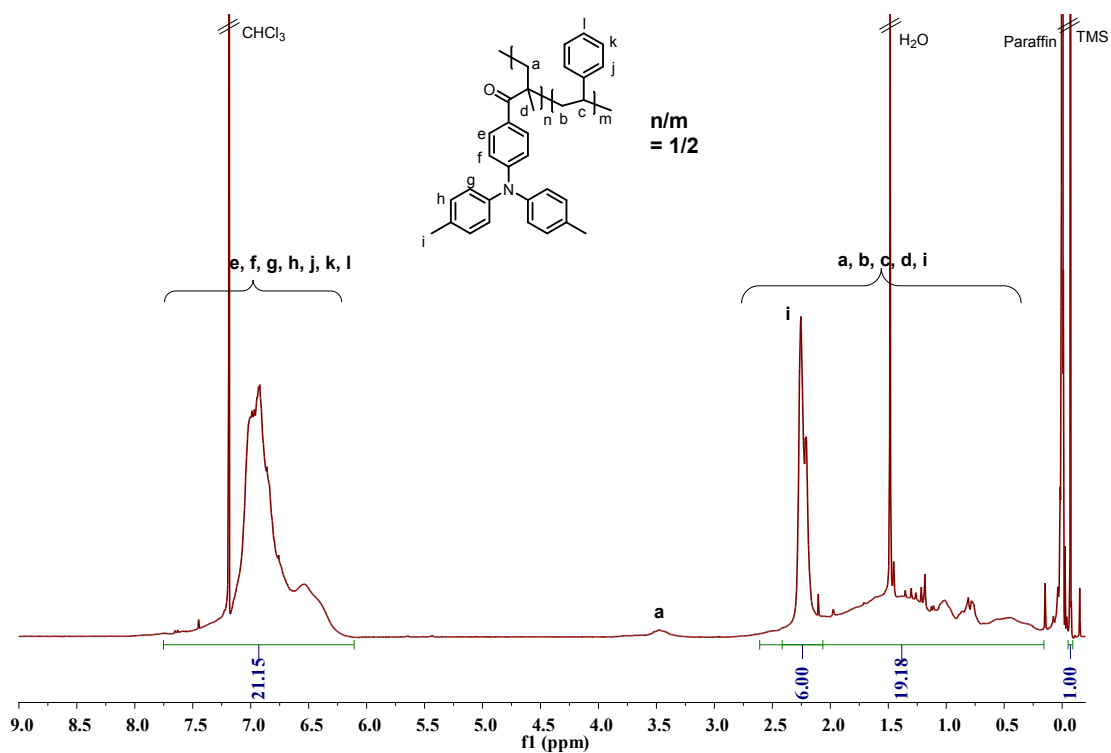
Fig. S7. ^{1}H NMR spectrum of poly(IMAPK-co-St) ([IMAPK]/[St] =1/2 in polymer). [400 MHz, CDCl$_3$, TMS, room temp.]
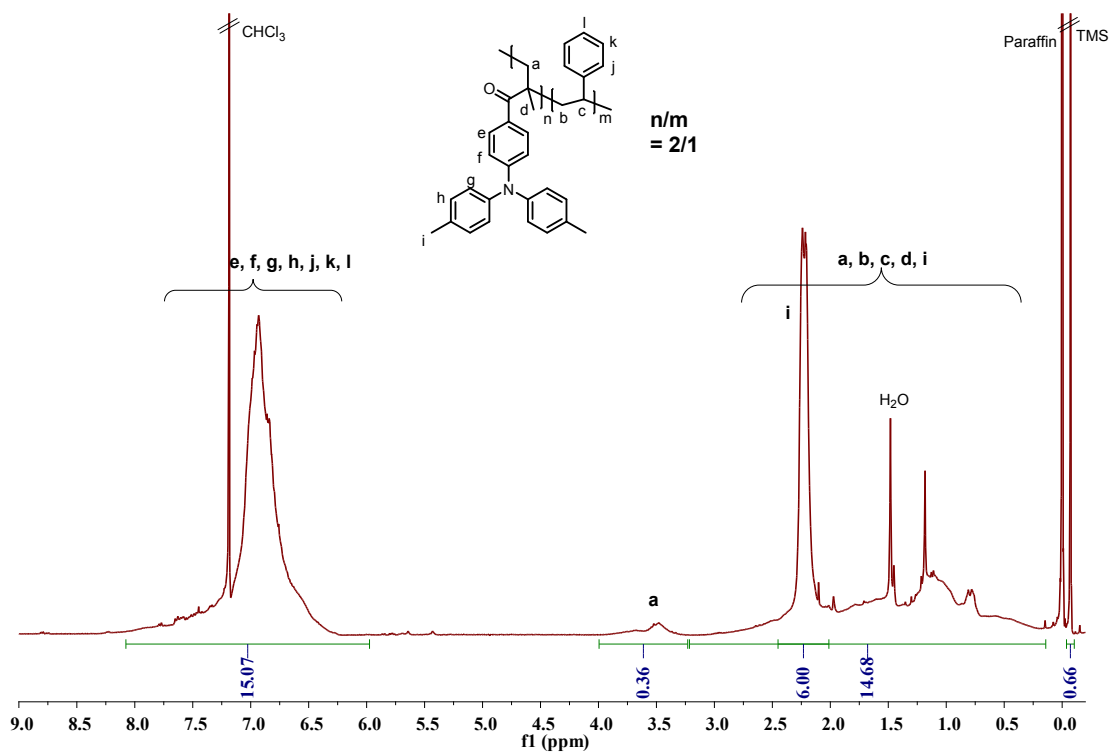
Fig. S8. ^{1}H NMR spectrum of poly(IMAPK-co-St) ([IMAPK]/[St] =2/1 in polymer). [400 MHz, CDCl$_3$, TMS, room temp.]
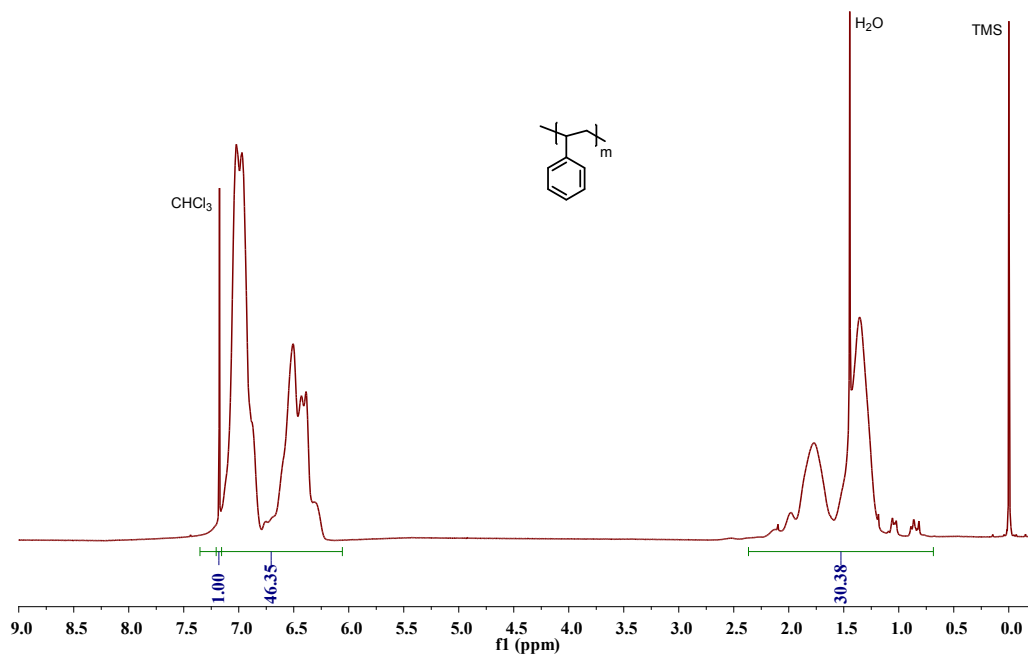
Fig. S9. ^{1}H NMR spectrum of poly(St) (run 7 in Table S1). [400 MHz, CDCl$_3$, TMS, room temp.]
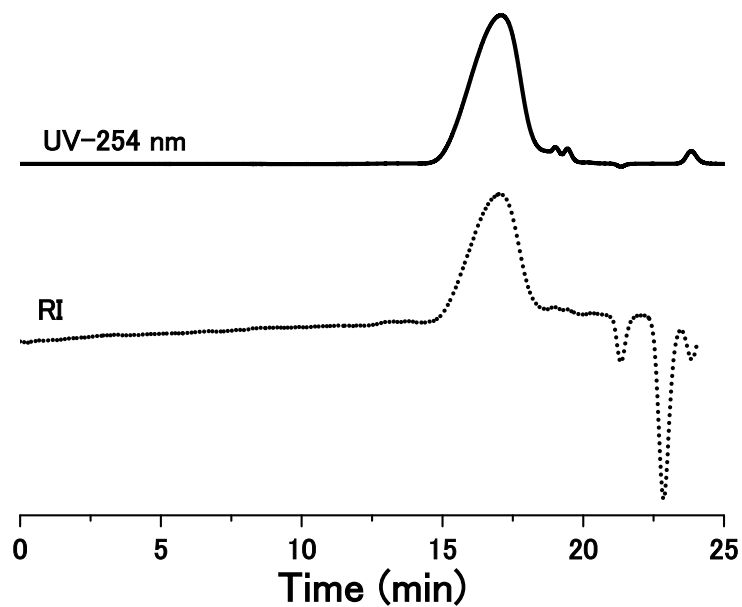
Fig. S10. SEC curves of poly(IMAPK-co-St) ([IMAPK]/[St] = 1/5).
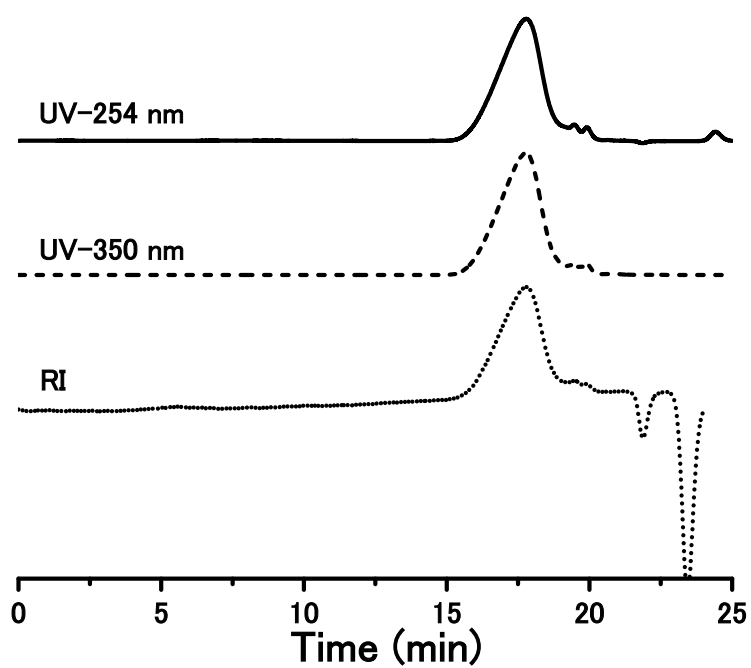
Fig. S11. SEC curves of poly(IMAPK-co-St) ([IMAPK]/[St] = 1/2).
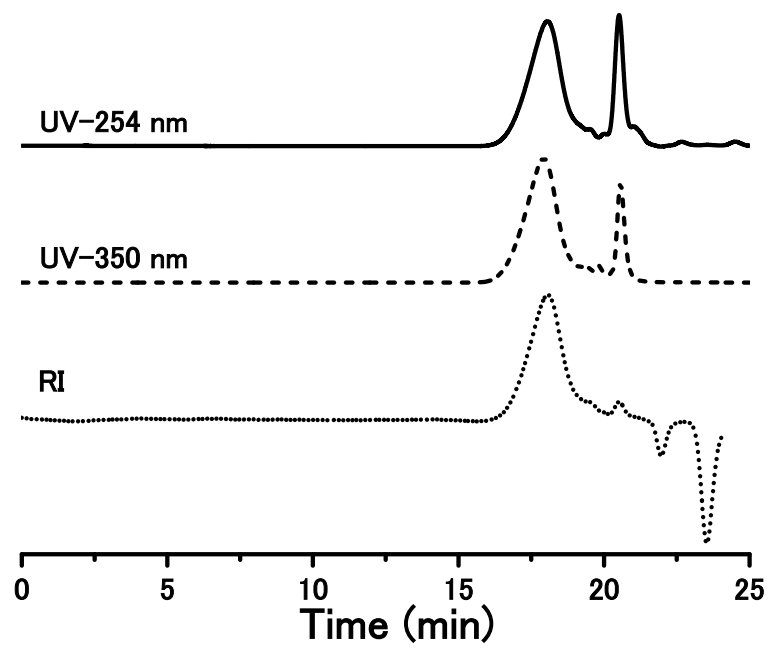
Fig. S12. SEC curves of poly(IMAPK-co-St) ([IMAPK]/[St] = 2/1).
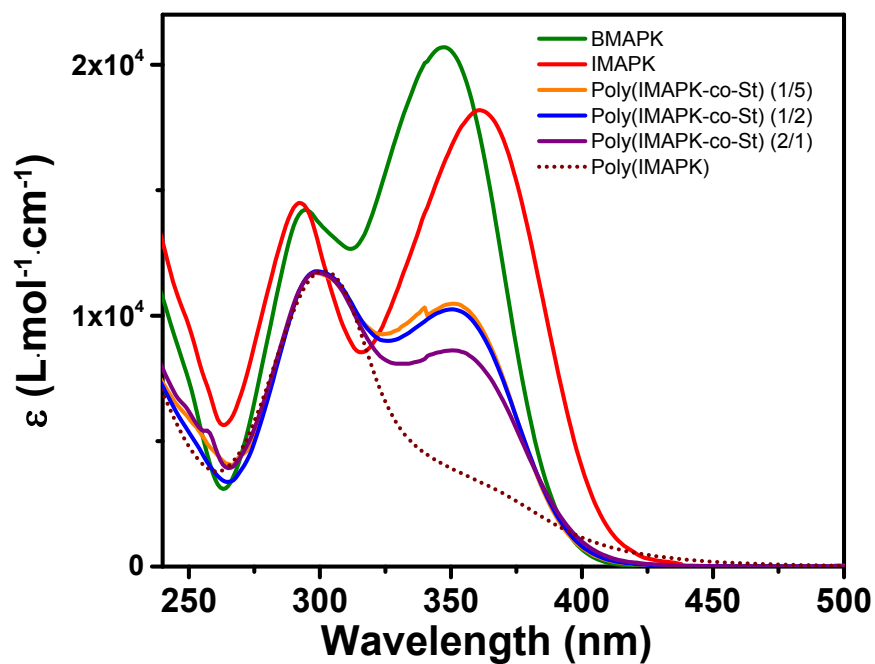
Fig. S13. UV-Vis spectra of BMAPK, IMAPK, poly(IMAPK-co-St)s, and poly(IMAPK) in THF. Concentration: ca. 3×10^{-5} mol/L, cell length: 10 mm.
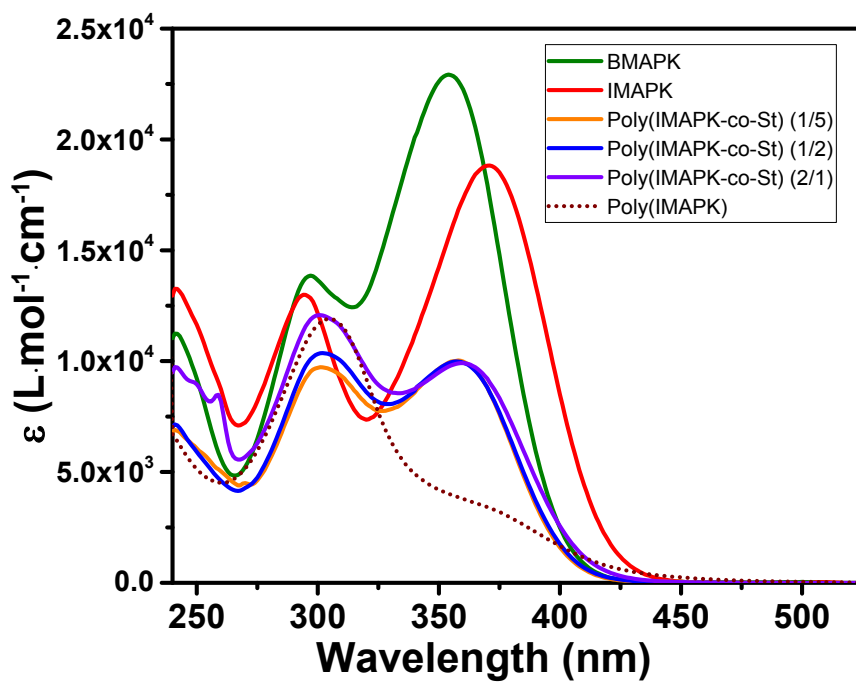
Fig. S14. UV-Vis spectra of BMAPK, IMAPK, poly(IMAPK-co-St)s, and poly(IMAPK) in chloroform. Concentration: ca. 3×10^{-5} mol/L, cell length: 10 mm.
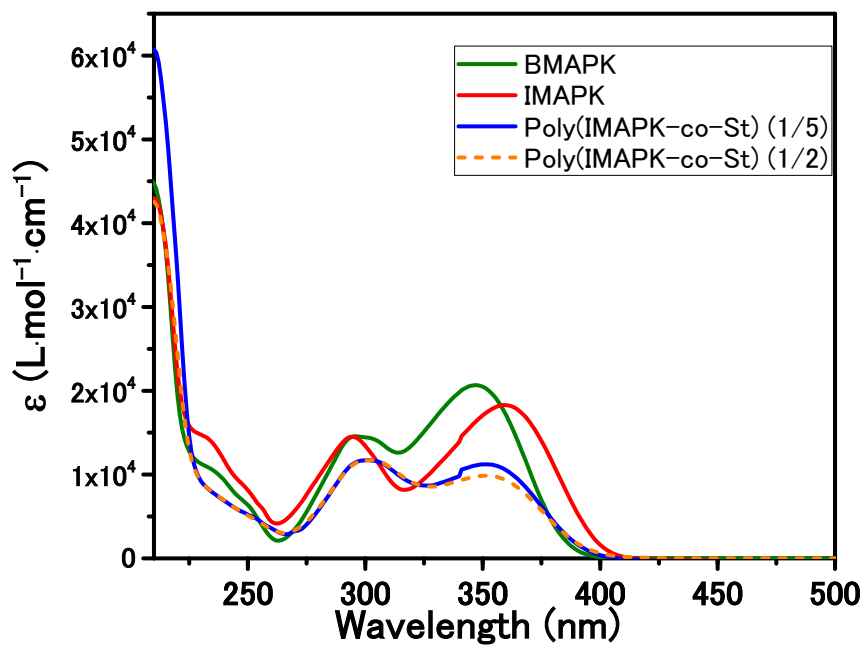
Fig. S15. UV-Vis spectra of BMAPK, IMAPK and poly(IMAPK-co-St)s ([IMAPK]/[St] = 1/5 and 1/2) in cyclohexane. Concentration: ca. 3×10^{-5} mol/L, cell length: 10 mm.
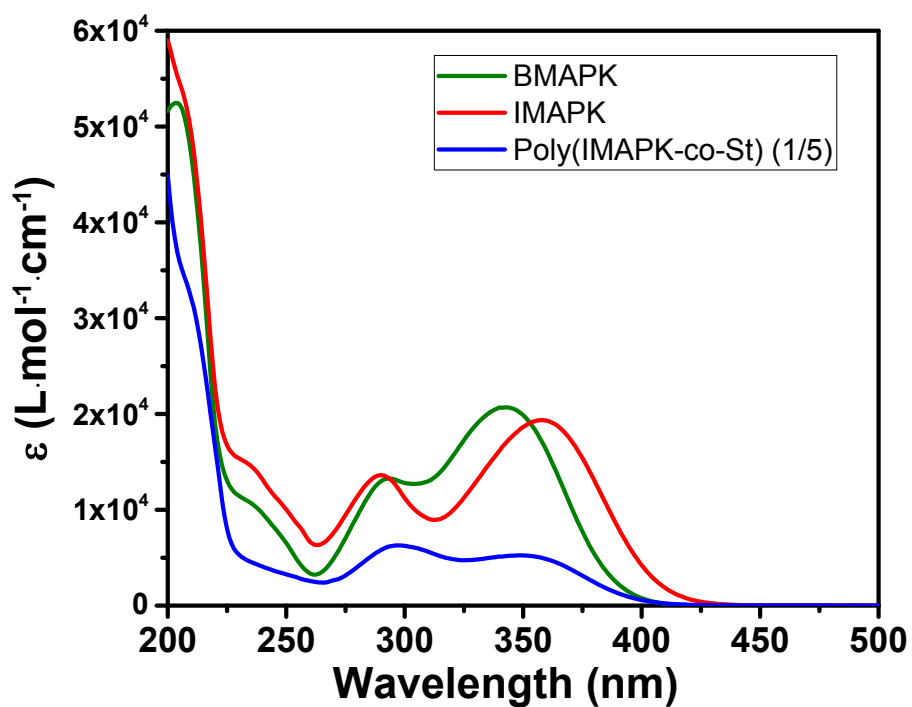
Fig. S16. UV-Vis spectra of BMAPK, IMAPK, and poly(IMAPK-co-St) ([IMAPK]/[St] = 1/5; normalized at 297 nm) in acetonitrile. Concentration: ca. 3×10^{-5} mol/L, cell length: 10 mm.
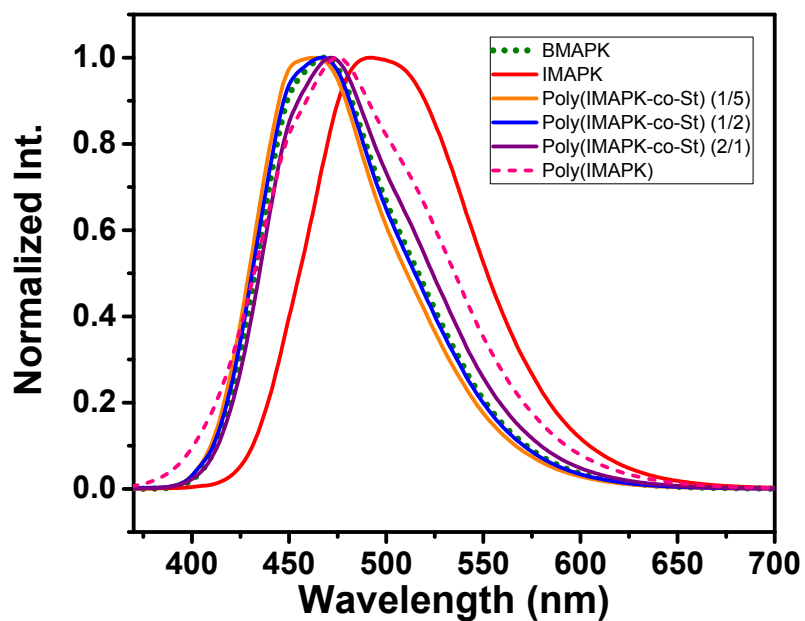
Fig. S17. Emission spectra of BMAPK, IMAPK, poly(IMAPK-co-St)s, and poly(IMAPK) in THF. Concentration: ca. 1×10^{-6} mol/L, excited wavelength: 360 nm, cell length: 10 mm.
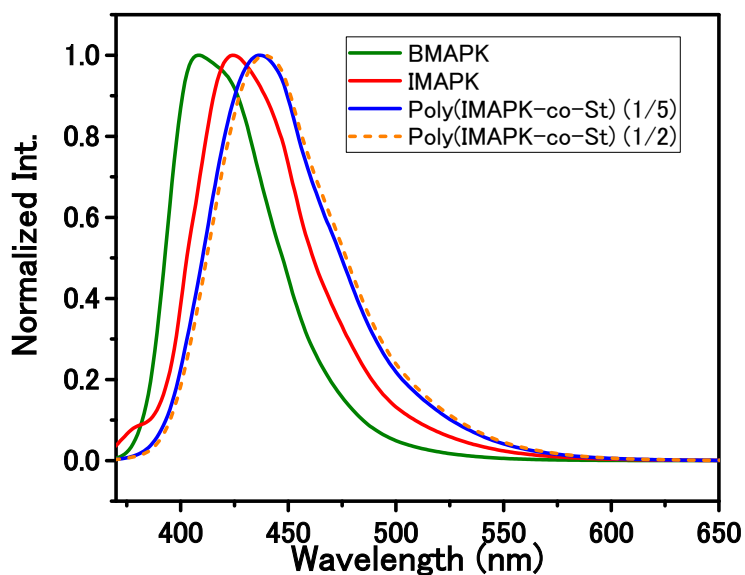
Fig. S18. Emission spectra of BMAPK, IMAPK and poly(IMAPK-co-St)s ([IMAPK]/[St] = 1/5 and 1/2) in cyclohexane. Concentration: ca. 1×10^{-6} mol/L, excited wavelength: 360 nm, cell length: 10 mm.
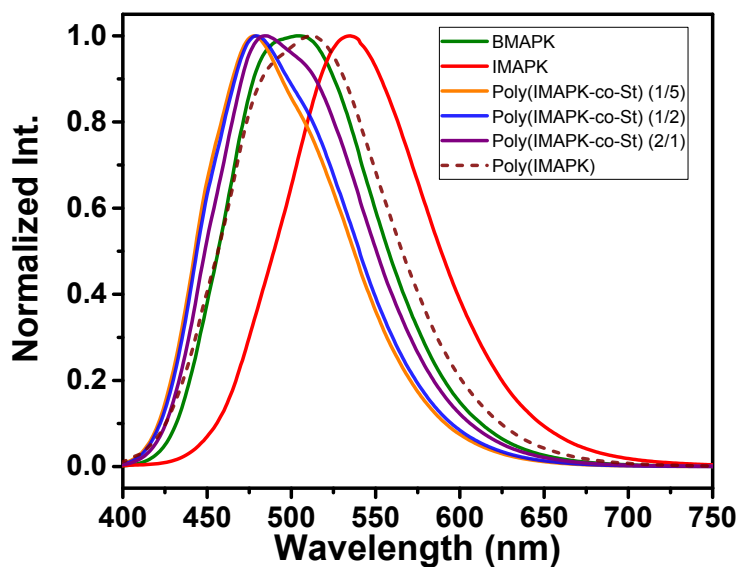
Fig. S19. Emission spectra of BMAPK, IMAPK, poly(IMAPK-co-St)s, and poly(IMAPK) in CHCl$_3$. Concentration: ca. 1×10^{-6} mol/L, excited wavelength: 360 nm, cell length: 10 mm.
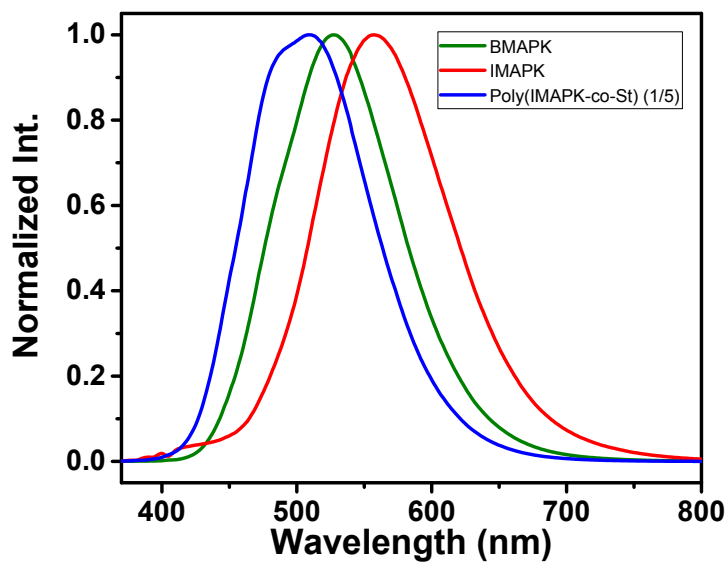
Fig. S20. Emission spectra of BMAPK, IMAPK, poly(IMAPK-co-St) ([IMAPK]/[St] = 1/5), and poly(IMAPK) in CH$_3$CN. Concentration: ca. 1×10^{-6} mol/L, excited wavelength: 360 nm, cell length: 10 mm.
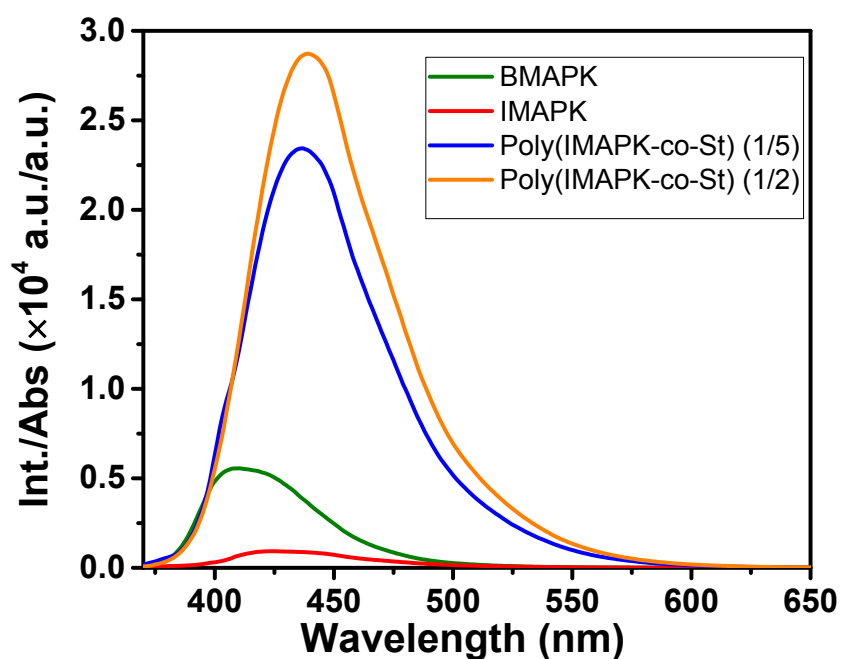
Fig. S21. Emission spectra of BMAPK, IMAPK and poly(IMAPK-co-St)s ([IMAPK]/[St] = 1/5 and 1/2) in cyclohexane. Emission intensity was normalized according to the corresponding absorption at excitation wavelength (360 nm).
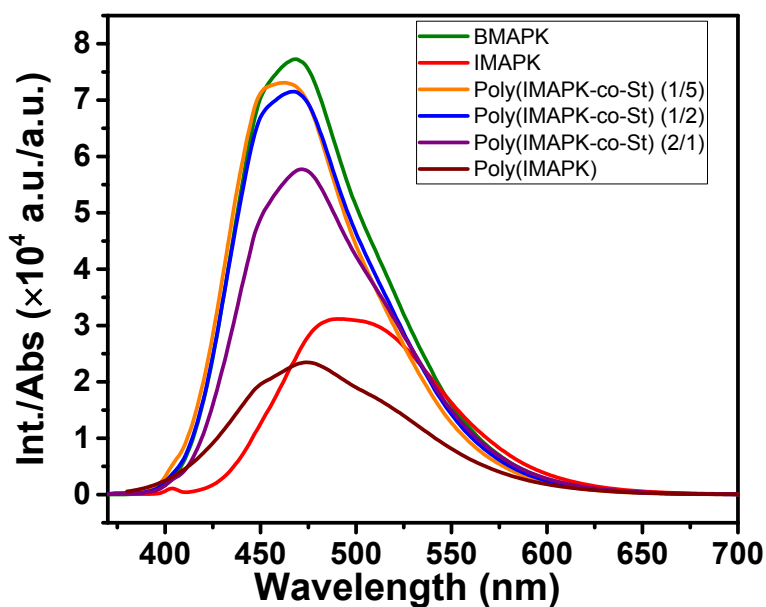
Fig. S22. Emission spectra of BMAPK, IMAPK, poly(IMAPK-co-St)s, and poly(IMAPK) in THF, emission intensity was normalized according to the corresponding absorption at excitation wavelength (360 nm).
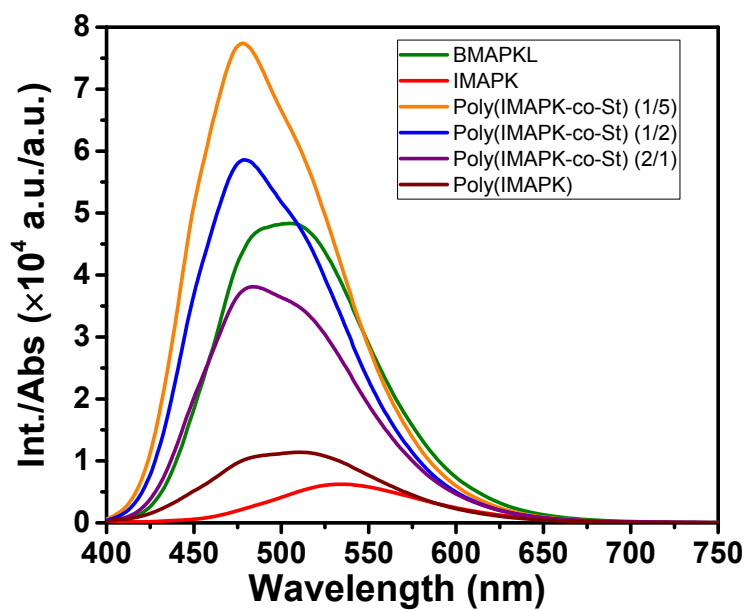
Fig. S23. Emission spectra of BMAPK, IMAPK, poly(IMAPK-co-St)s, and poly(IMAPK) in CHCl₃, emission intensity was normalized according to the corresponding absorption at excitation wavelength (360 nm).
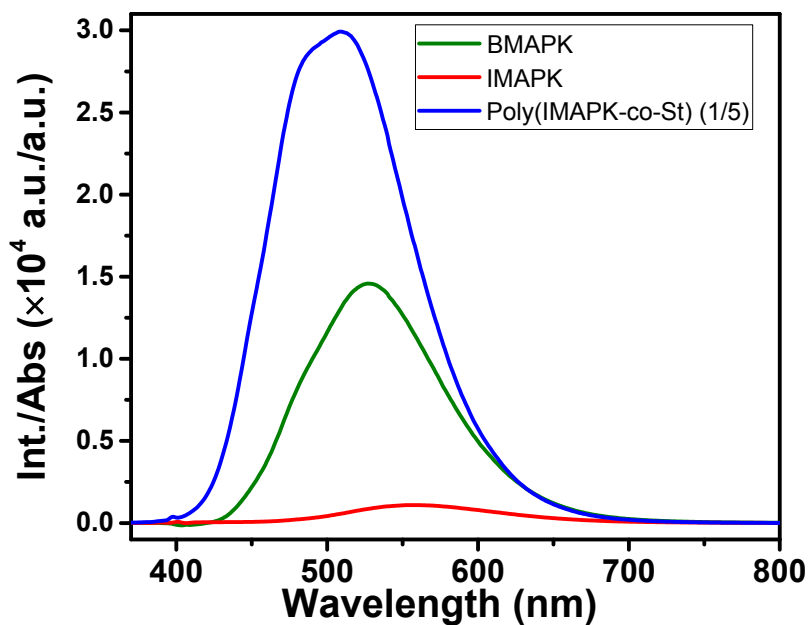
Fig. S24. Emission spectra of BMAPK, IMAPK, and poly(IMAPK-co-St) ([IMAPK]/[St] = 1/5) in CH₃CN, emission intensity was normalized according to the corresponding absorption at excitation wavelength (360 nm).
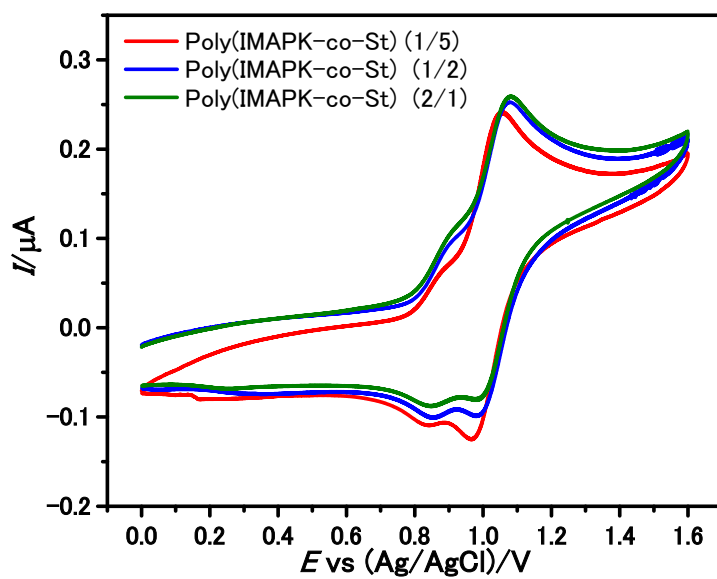
Fig. S25. CVs of poly(IMAPK-co-St)s ([IMAPK]/[St] = 1/5, 1/2, and 2/1) recorded in CH_2Cl_2 solutions (ca. 1 mM) containing 0.1 M TBAH at a scanning rate of 100 mV/s.
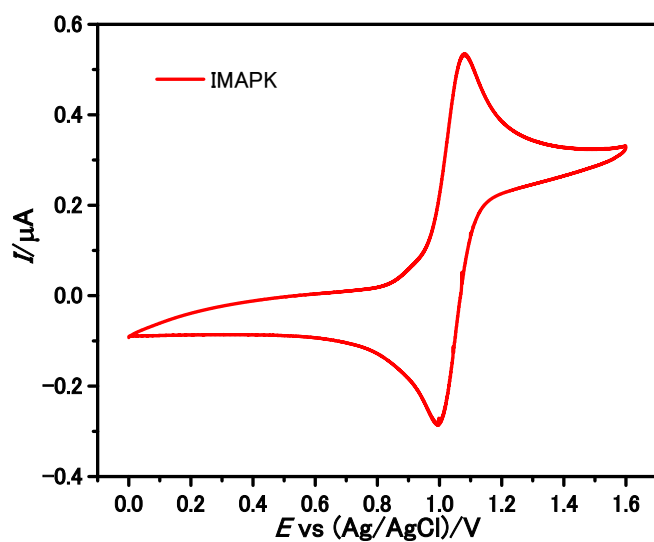
Fig. S26. CVs of IMAPK recorded in CH_2Cl_2 (ca. 1 mM) containing 0.1 M TBAH at a scanning rate of 100 mV/s.

(A) HOMO (-8.38 eV)
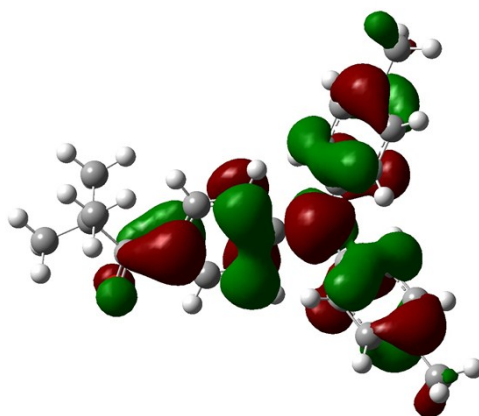
(B) LUMO (-5.88 eV)
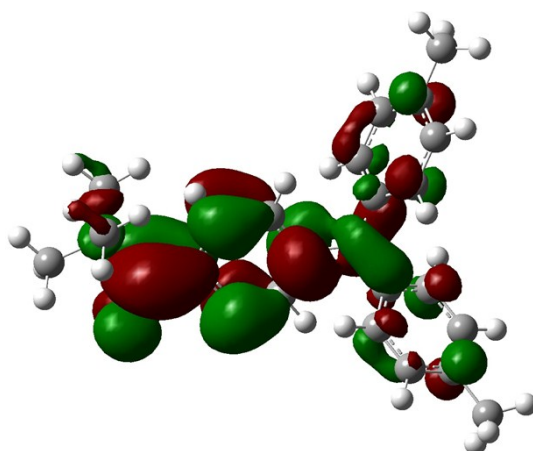
(C) LUMO+1 (-5.40 eV)
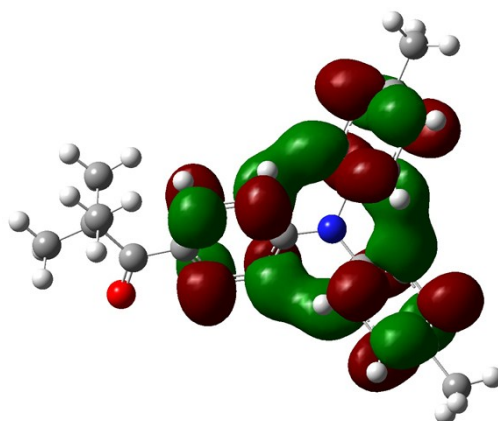
Fig. S27. Optimized geometry with HOMO (A), LUMO (B),and LUMO+1 (C) orbitals of BMAPK calculated by DFT in the ground state at the B3LYP/6-311G(d, p) level.

(A) HOMO (-8.30 eV)
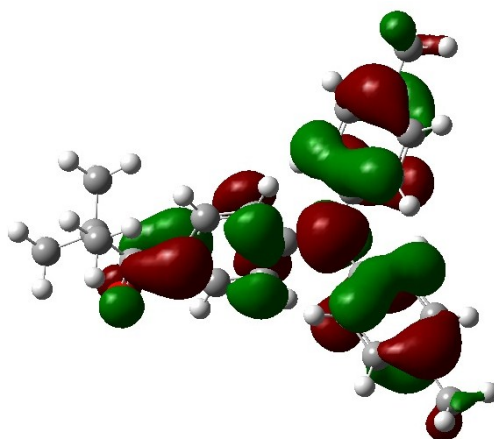
(B) LUMO (-6.19 eV)
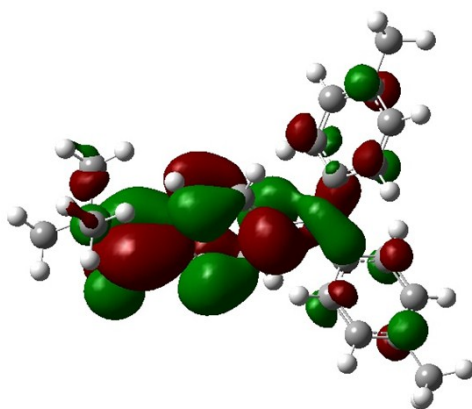
(C) LUMO+1 (-5.36 eV)
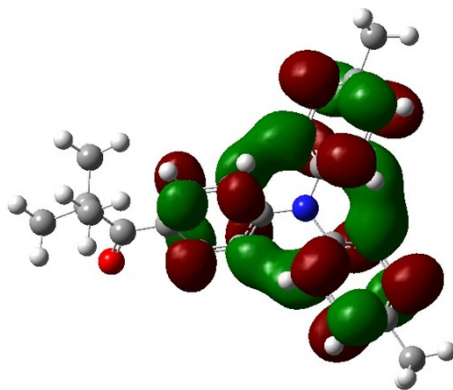
Fig. S28. Optimized geometry with HOMO (A), LUMO (B),and LUMO+1 (C) orbitals of BMAPK calculated by TD-DFT in the lowest-energy excited state at the B3LYP/6-311G(d, p) level.
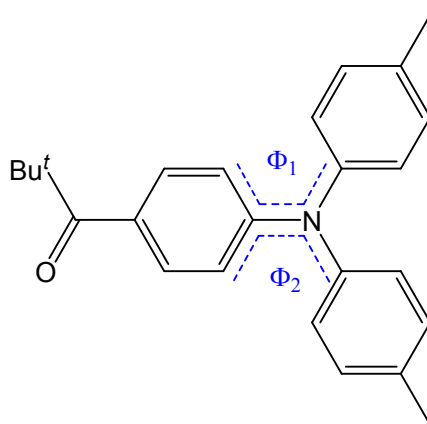
$\Phi_1 = -29.4^\circ$ (ground state), -43.6° (lowest-energy excited state)
$\Phi_2 = -30.1^\circ$ (ground state), -42.7° (lowest-energy excited state)

Averaged dihedral angle = -29.8° (ground state), -43.2° (lowest-energy excited state)

Fig. S29. Structures of BMAPK with dihedral angles definitions. The averages of Φ_1 and Φ_2 are taken as dihedral angles around the single bond connecting the carbonylphenyl group and the N atom in the ground state and in the lowest-energy excited state.

(A)

INTENSITY-Weighted GAUSSIAN DISTRIBUTION Analysis (Solid Particle)

GAUSSIAN SUMMARY:

Mean Diameter   = 106.8 nm   Chi Squared   = 72.703
Stnd. Deviation = 42.5 nm (39.8 %) Baseline Adj.   = 0.000 %
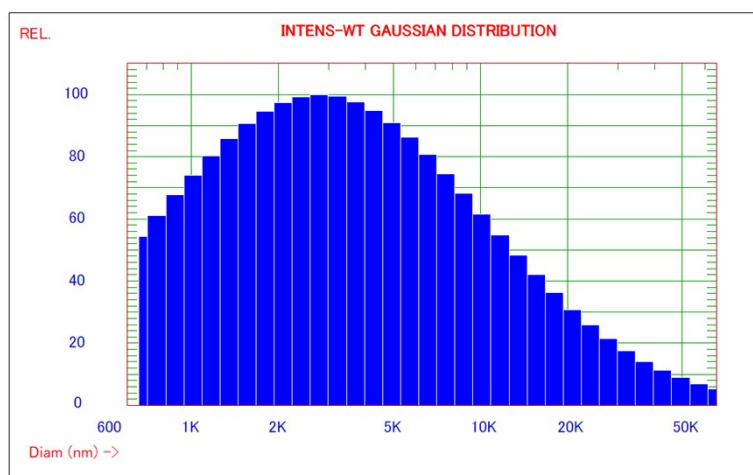Coeff. of Var'n = 0.398   Mean Diff. Coeff. = 1.00E-007 cm2/s
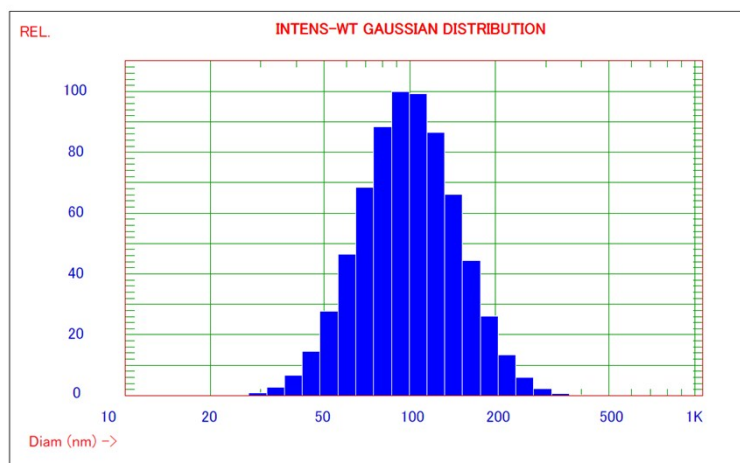
(B)

INTENSITY-Weighted GAUSSIAN DISTRIBUTION Analysis (Solid Particle)

GAUSSIAN SUMMARY:

Mean Diameter   = 6584.1 nm   Chi Squared   = 193.287
Stnd. Deviation = 8625.2 nm (131.0 %) Baseline Adj.   = 0.011 %
Coeff. of Var'n = 1.310   Mean Diff. Coeff. = 7.37E-010 cm2/s
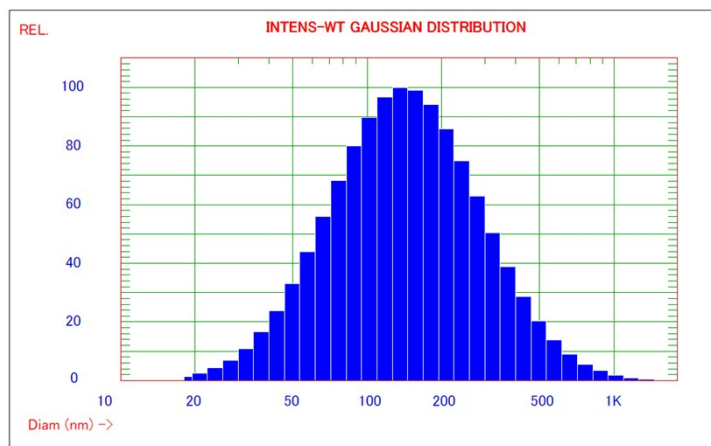

Fig. S30. Particle size distributions of poly(IMAPK-co-St) ([IMAPK]/[St] = 1/2) in THF (A) and in cyclohexane (B) obtained by dynamic light scattering.   Concentration = 0.5 mol/L (per monomeric residue).
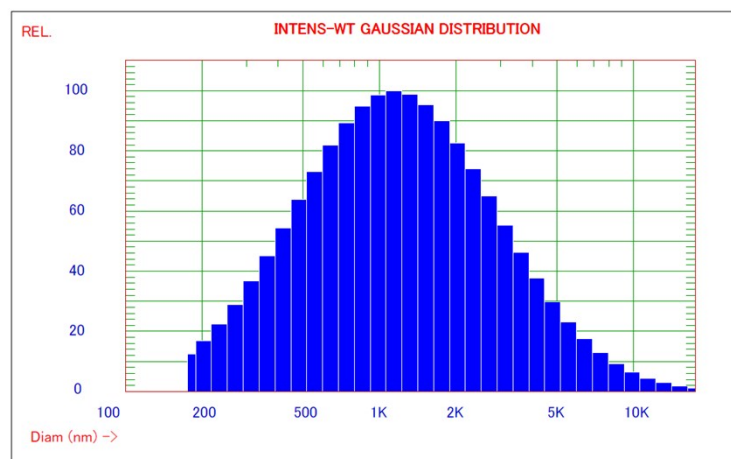
Fig. S31. Particle size distributions of poly(IMAPK-co-St) ([IMAPK]/[St] = 1/5) in THF (A) and in cyclohexane (B) obtained by dynamic light scattering.　　Concentration = 0.5 mol/L (monomeric residue).

References:

1) S. Hamai, F. Hirayama, *J. Phys. Chem.* **1983**, *87,* 83-89.